RESEARCH ARTICLE

Boronic acid treatment phenocopies *monopteros* by affecting PIN1 membrane stability and polar auxin transport in *Arabidopsis thaliana* embryos

Michaela Matthes[‡] and Ramón A. Torres-Ruiz*,[§]

ABSTRACT

Several observations suggest that the micronutrient boron (B) has a stabilising role in the plasma membrane (PM), supporting functions in PM-linked (hormone) signalling processes. However, this role is poorly characterised. Here we show treatment with boronic acids, specific competitors of B, phenocopies the *Arabidopsis thaliana* rootless pattern mutant *monopteros*. At least in part, this is caused by phenylboronic acid (PBA)-induced internalisation of the membrane-localised auxin efflux carrier PINFORMED1 (PIN1) in the early embryo. PIN1 internalisation interrupts the feedback signal transduction cascade involving the phytohormone auxin, PIN1 and the transcription factor gene *MONOPTEROS*. This entails several effects, including abnormal development of vascular cell precursors, suppression of *MONOPTEROS* downstream targets and loss of the root auxin maximum – essential signals for root meristem development. While PIN1 is internalised, we observe a differential effect of PBA on other proteins, which are either unaffected, internalised or, as in the case of the B transporter BOR1, stabilised at the PM. These findings suggest a competition of PBA with B for plant membrane proteins and might shed light on the function of B at the PM.

KEY WORDS: Boron, Boronic acid, Plasma membrane, *Arabidopsis*, MONOPTEROS, PINFORMED1, PIN1, ENHANCER OF PINOID

INTRODUCTION

The micronutrient boron (B) is essential for many organisms (Kliegel, 1980). Membrane-localised transporters in plants and animals control B homeostasis (Takano et al., 2002; Park et al., 2004; Tanaka et al., 2008; Durbak et al., 2014) and act to counteract the detrimental effects that B excess or depletion can have for plants and animals (Warington, 1923; Sommer and Sorokin, 1928; Lanoue et al., 1998; Rowe and Eckhert, 1999; Goldbach et al., 2001; Fort et al., 2002; Reid et al., 2004; Nielsen, 2008; Martin-Rejano et al., 2011; Abreu et al., 2014). Consequently, the concentration of B in soils, whether high or low, is of considerable importance for crop production (Dell and Huang, 1997; Shorrocks, 1997; Reid et al., 2004; Durbak et al., 2014).

The key to understanding the molecular functions of B, in the form of boric acid $B(OH)_3$ or borate anions $B(OH)_4^-$, is its reactivity with (two) *cis*-diol pairs and its capability to form (ester) cross-links between neighbouring molecules through their *cis*-diol moieties (Kliegel, 1980; Brown et al., 2002; Bolaños et al., 2004). Experimental analysis has often explored the reaction of organisms under low B concentration (see aforementioned citations). This is challenging because B-free experimental conditions cannot be attained to completion because B is ubiquitous. As a simpler approach, the use of boronic acids, such as phenylboronic acid (PBA), has emerged as an alternative to imitate B depletion conditions (Bassil et al., 2004). Boronic acids and their boronates are specific B competitors with the same binding specificity as boric acid but that cannot serve to cross-link two molecules because they only have one hydroxyl pair (e.g. Torssell, 1963), a feature used in boronate-affinity chromatography (e.g. Wimmer et al., 2009).

In spite of this long history, the mechanistic role of B is understood in only few processes; for instance, as a component of the bacterial quorum sensor (Chen et al., 2002) and in plant cell wall stabilisation through cross-linking rhamnogalacturonan-II polysaccharides (Ishii and Matsunaga, 1996; Kobayashi et al., 1996; O'Neill et al., 1996). However, the fact that B is required in plants as well as in animals suggests roles beyond cell wall stabilisation. One hypothesis is that B might be required for the stability of plasma membrane (PM) proteins, which control key processes in physiology and morphogenesis, for instance by cross-linking glycoproteins and/or lipids (Parr and Loughman, 1983; Brown et al., 2002; Bassil et al., 2004; Goldbach and Wimmer, 2007). In fact, numerous B depletion- or boronic acid-induced phenomena affect morphogenesis and organogenesis processes, which are likely to depend on PM-relayed signal transduction pathways, such as root growth and root apical meristem (RAM) development (Sommer and Sorokin, 1928). Prominent in plants is the PBA-induced monocotyly in the dicot *Eranthis hyemalis* (Haccius, 1960). The reason for this remains unknown, most likely because this plant has a special mode of embryo development that takes place during germination and requires several months. Exploring a possible B-related morphogenetic process in plant embryos, we detected that boronic acids are capable of inducing phenocopies of the *Arabidopsis thaliana* rootless pattern mutant *monopteros* by interruption of polar auxin transport. The data show that PBA affects the membrane stability of proteins such as PIN1.

RESULTS

PBA induces phenocopies of *A. thaliana MONOPTEROS* mutants

We detected that treatment of siliques of different *A. thaliana* accessions with PBA produced up to 98% (per silique) rootless seedlings, whereas controls gave only wild-type seedlings (Fig. 1, Table S1). The rootless seedlings were highly similar to mutants of the transcription factor *MONOPTEROS* (*MP*) based on morphological

Lehrstuhl für Genetik, Technische Universität München, Wissenschaftszentrum Weihenstephan, Emil-Ramann-Str. 8, Freising D-85354, Germany.
*Present address: Entwicklungsbiologie der Pflanzen, Technische Universität München, Wissenschaftszentrum Weihenstephan, Emil-Ramann-Str. 4, Freising D-85354, Germany. ‡Present address: Division of Biological Sciences, Bond Life Sciences Center, Interdisciplinary Plant Group, University of Missouri, Columbia, MO 65211, USA.

§Author for correspondence (ramon.torres@wzw.tum.de)

The Company of Biologists

DEVELOPMENT

and histological criteria. Both displayed occasionally irregular cotyledons, severe defects of the vascular system, little hypocotyl with large vacuolated and few epidermal cells and complete absence of the RAM (Fig. 1A-D). Only a few seedlings were lethal or stunted. A few others displayed longer hypocotyls lacking RAMs or abnormal cotyledon number and size, suggesting late or incomplete contacts of embryos with PBA (<3%; Fig. S1). In order to exclude indirect effects of silique physiology (e.g. upon metabolising PBA), isolated ovules with embryos up to the heart stage were PBA treated and cultured according to Sauer and Friml (2004). Up to 44% of all embryos (n=35; water-treated controls, 0%) of late heart stage and beyond were identified as phenocopies (Fig. 1E,F). For convenience, we use the term '*monopteros* (*mp*) phenocopies' hereafter.

Structural peculiarities of boronic (and boric) acids may impact their capability to penetrate tissues and to induce *mp* phenocopies

Binding affinities of boronic acids can depend on various chemical parameters, in particular different substituents (Fig. 2A) (Yan et al., 2004). Testing 3-methoxyphenylboronic acid

Fig. 1. Comparison of *mp* mutants and *mp* phenocopies. (A) *A. thaliana mp* mutants, wild type (WT) and *mp* phenocopies (ph.copy). Specimens of the different groups (as separated by the black lines) are arranged side by side for comparison (compilation from a larger picture). (B) Clearing preparations of *mp* mutants and *mp* phenocopies with defect vascular elements (arrowheads). Each single seedling image (as separated by the white lines) is a composite of higher magnification images. The inset shows a wild-type seedling (composite image). (C) Electron micrographs of *mp* (left) and phenocopy (right). (D) Basal region sections of two *mp* mutants (left) and two *mp* phenocopies (right). Arrowheads point to epidermal-like cells. (E) Comparison of heart stage embryos from ovule culture of wild type (left) and two PBA-induced *mp* phenocopies (middle and right). (F) As E, but torpedo stage embryos of wild type (left) and *mp* phenocopy (right). Scale bars: 1 mm in A; 100 µm in B,D; 200 µm in inset of B; 500 µm in C; 20 µm in E,F.

(3-MPBA), 4-methoxyphenylboronic acid (4-MPBA) and 3-nitrophenylboronic acid (3-NPBA) demonstrated their capability to induce *mp* phenocopies with variable frequencies: a maximum of 78%, 100% and 100% phenocopies per silique, respectively (Fig. 2B, Fig. S1, Table S1; the abbreviations are for convenience and do not necessarily conform with any chemical convention). In view of these results, we tested the structurally unrelated butylboronic acid (BBA), which has a non-phenolic substituent (Fig. 2A). In fact, BBA treatment of siliques produced 2% phenocopies at most (Fig. 2B, Table S1). By introducing a lateral opening in the siliques (see the Materials and Methods) only a maximum of 35% *mp* phenocopies per silique was achieved (Table S1, Fig. S1). The BBA frequency remained low in embryos from ovule culture (Fig. S2) in spite of using a tenfold higher concentration in comparison to PBA (8%, n=128; water-treated controls, 0%).

The known chemical competition of B (boric acid) versus boronic acids for *cis*-diols suggests that one should outcompete the other if present in excess. However, elevated concentrations of boric acid (120 mM, 150 mM) failed to suppress the effect of low (10 mM) PBA concentrations in several experiments (as compared with PBA alone; Table S2). At the same time, application of the same amounts of boric acid alone did not affect the seedling morphology (Table S2). From the silique treatments, ovule culture and competition experiments we therefore concluded that the structure of boric and boronic acids affects the capacity to penetrate tissues and to induce *mp* phenocopies.

The ability of boronic acids to induce *mp* phenocopies lies in the boronic acid moiety

Boronic acids share structural similarity to acetic and benzoic acid compounds (Fig. 2A). Acetic acids have been used to verify that the effects of boronic acids are specifically due to the disruption of B cross-links and not to other general effects (Bassil et al., 2004). After application of phenylacetic acid (PAA), 3-methoxyphenyl-, 4-methoxyphenyl- and 3-nitrophenylacetic acid most seedlings had a wild-type appearance, except in 14/265 siliques, where 1.8-35% cotyledon fusions were found (Fig. S3, Table S3). This is compatible with the fact that PAA is known to be a 'mild auxin' in other plants (Simon and Petrásek, 2011). All treatments failed to produce *mp* phenocopies. Note that at least one of these compounds (3-nitrophenylacetic acid) is a much stronger acid than PBA, 4-MPBA or 3-NPBA (Bassil et al., 2004). In addition, experiments with benzoic acid, 3-methoxybenzoic, 4-methoxybenzoic and 3-nitrobenzoic acid produced predominantly wild-type progeny. No *mp* phenocopies were generated. Other seedlings germinated but were growth retarded, displayed malformed apices or short roots with regular cell files. Notably, defective seedlings occurred in all siliques, excluding an effect on a particular developmental stage (Table S4). The aforementioned results showed that every boronic acid tested is capable of inducing *mp* phenocopies. Together with the (negative) results obtained with acetic and benzoic acids, this shows that the boronic acid moiety alone is responsible for *mp* phenocopy induction.

Boronic acid-treated embryos fail to correctly execute the first formative cell division of the hypophysis leading to RAM generation

mp phenocopy induction did not depend on the accession/line or whether siliques grew on primary or secondary stems. It rather occurred in siliques harbouring early embryo stages (Fig. 2B, Fig. S4, Table S1). This suggested that embryos up to early torpedo
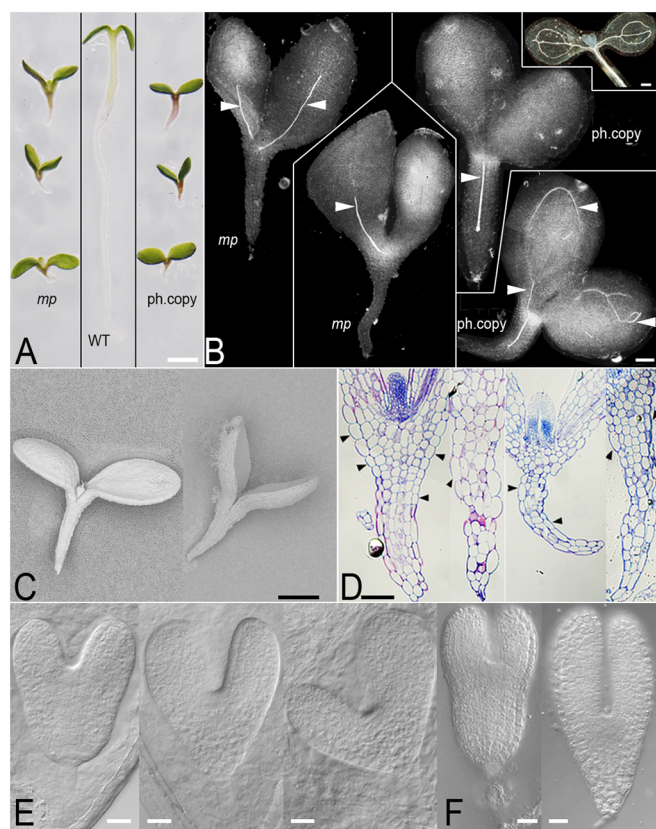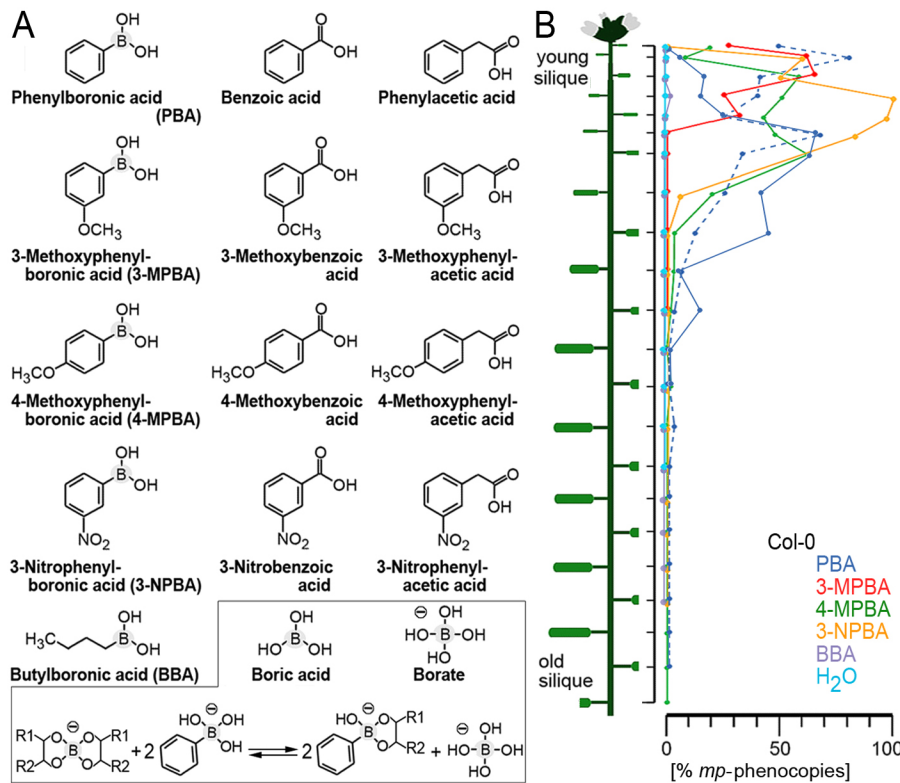
Fig. 2. Effect of boronic acids on *A. thaliana* embryo development. (A) Structure of the tested boronic, benzoic and acetic acids, boric acid and borate. Borate, PBA and *cis*-diol reactions are shown at the bottom. (B) Representative frequencies of *mp* phenocopies (Col-0 background) per silique. Solid lines indicate single treatment; dashed line indicates PBA treatment once a day on five consecutive days. Treated stems/branches had different numbers of siliques. Solutions were 50 mM or saturated, with water as control.

stage responded to the boronic acid treatment, since these stages are crucial for forming the RAM (Jürgens and Mayer, 1994). RAM formation starts with a horizontal division of the hypophysis cell in *A. thaliana* (Schlereth et al., 2010). With this in mind, all siliques of selected branches were treated with PBA and the embryos of every silique were separately evaluated after 24 h. Thus, for every silique,

the frequency of embryos corresponding to a particular stage subdivided into the frequencies (%) of normal embryos and of embryos displaying abnormal cell divisions were scored (Fig. 3A, Table S5). For instance, the third silique of a treated Col-0 plant (in Fig. 3A) produced 22% and 7% abnormal early and mid heart stage embryos, respectively (white box, red squares). In addition, the
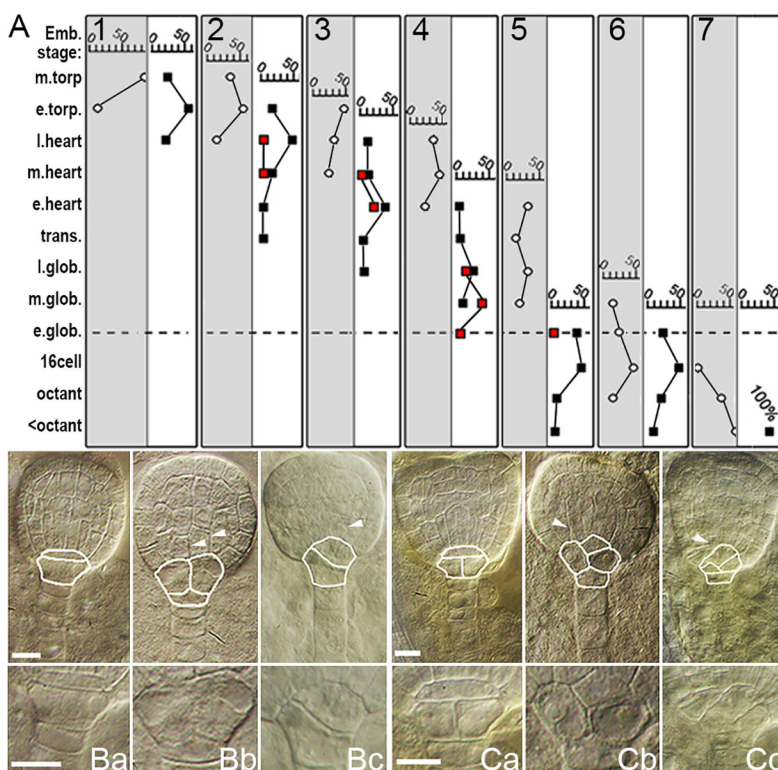

Fig. 3. PBA interferes with the formative division of the hypophysis. (A) Embryo stage frequencies in two Col-0 plants with seven siliques on the primary stem, from oldest (1) to youngest (7), with plant/siliques untreated (left, grey) versus plant/siliques 24 h after PBA treatment (right, white). The upper bar in each box (0% and 50% indicated) gives the percentage of isolated wild-type embryo stages per silique in the untreated plant (white circles) and the percentage of isolated wild-type and *mp* phenocopy embryo stages per silique in the PBA-treated plant (black and red squares, respectively). Dashed line indicates the stage with earliest defects in the hypophysis. (B,C) Wild-type (a), *mp* phenocopy (b) and *mp* (c) embryos at early globular (B) and late globular (C) stages. The bottom row shows higher magnifications of the hypophysis. Arrowheads point to central cells with altered proportions as compared with central elongated cells in wild types. White lines aid recognition of hypophysis descendants. Glob, globular; trans, transition; torp, torpedo; e, early; m, mid; l, late. Scale bars: 10 µm.

same silique gave normal embryos of the late globular (7%), transition (4%), early heart (39%), mid heart (11%) and late heart (11%) stages (white box, black squares). The third silique of a comparable untreated plant produced only wild-type embryos (grey box, white circles). In this way, the effect of PBA could be traced back to the early (32-cell) globular stage as a deviation from the first formative division of the hypophysis resembling that observed in *mp* mutants (Fig. 3Ba-c,Ca-c). Vascular precursor cells could also display abnormal morphologies, being less elongated along the apical-basal axis of the embryo (Fig. 3B,C).

Boronic acid-induced *mp* phenocopies lack essential signals for hypophysis formative division and RAM generation

Next, we focussed on the two signals known to trigger the formative division of the hypophysis, namely the accumulation of IAA (basal auxin maximum) and the presence of the mobile TARGET OF MONOPTEROS 7 (TMO7) transcription factor (Benková et al., 2003; Schlereth et al., 2010). We considered that boronic acids could bind *cis*-diols of nucleic acids and thus interfere with gene expression processes. However, RT-PCR analyses revealed no significant differences in the expression of *MP*, the *MP* repressor *BDL* or *ACTIN2* in *mp* phenocopies versus control seedlings (Fig. 4A, Fig. S5A). By contrast, boronic acid-induced *mp* phenocopies showed a severe reduction, if not a complete absence, of *TMO7* transcripts, as in *mp* and *bdl* mutants. All controls displayed strong *TMO7* expression (Fig. 4A). We concluded that boronic acid treatment does not generally affect transcription at this stage but specifically and indirectly that of *TMO7*.

Transcriptional differences of *TARGET OF MONOPTEROS 5* (*TMO5*), which is required for vascular development (De Rybel et al., 2013), were less pronounced (Fig. 4A). In this case, analyses
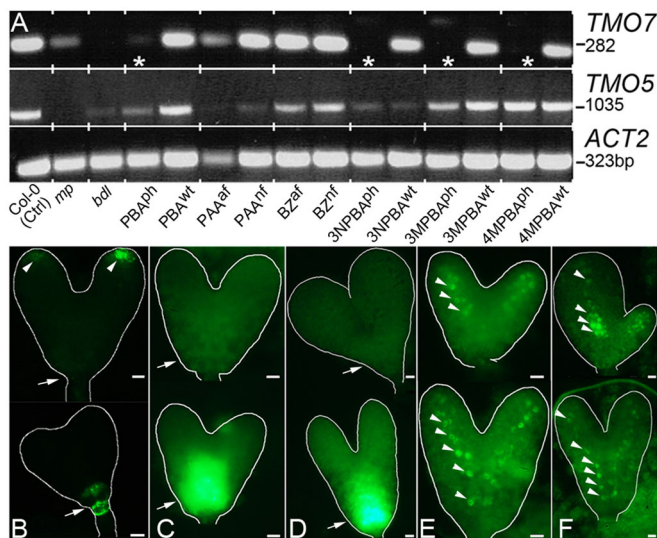

Fig. 4. Hypophysis signals in PBA-treated embryos. (A) RT-PCR with *TMO7*, *TMO5* and *ACT2* primers. Col-0 (Ctrl), mutant *mp* and *bdl* and *mp* phenocopies (ph) are compared with non-affected wild-type seedlings (wt) after treatment with PBA, 3-NPBA, 3-MPBA or 4-MPBA; and affected (af) versus non-affected (nf) seedlings are compared after PAA and benzoic acid (BZ) treatments. Note the effect on *TMO7* in *mp* phenocopies (stars). (B-F) PBA-treated (top) versus control (bottom) heart stage (B,C,E) and early torpedo stage (D,F) embryos. (B) DR5:GFP construct. (C,D) TMO7-3XGFP construct. (E,F) TMO5-3XGFP construct. Arrows point to the root tip; arrowheads point to GFP concentrations. White lines outline the embryos. Scale bars: 10 µm.

of reporter constructs, including *TMO5p:TMO5-3XGFP*, were more informative. We applied conventional epifluorescence in order to capture the complete fluorescence of the embryos. Upon PBA treatment, heart stage embryos carrying the IAA-responsive *DR5:: GFP* reporter displayed significantly reduced (45%) or absent (43%) root auxin maxima while simultaneously retaining the cotyledon tip maxima after 24 h (Fig. 4B; n=65; signal present in all controls). In *TMO7p:TMO7-3XGFP* embryos the threefold GFP fusion blocks mobility and shows where TMO7 originates. Here, TMO7-3XGFP could be severely altered, reduced or completely absent in embryos at 24 h or 48 h after PBA treatment (Fig. 4C,D; for statistics see Fig. S5B,C). Analysis of PBA-treated embryos carrying *TMO5p:TMO5-3XGFP*, which is visible in vascular precursor cells of cotyledons and the hypocotyl, displayed a mild but detectable delay of TMO5-3XGFP signal emergence around the heart stage (Fig. 4E,F; for statistics see Fig. S5D,E). Note that after 48 h embryos can be morphologically identified as *mp* phenocopies (Fig. 4D,F). Ovule culture experiments revealed essentially the same results for embryos carrying *DR5:GFP* and *TMO7p:TOM7-3XGFP* reporters (GFP signal absent in n=5/18 and 12/39, respectively; signal present in all controls; Fig. S6).

PBA causes internalisation of the IAA-related proteins PIN1 and ENP

In the embryo, the basal polarity of PIN1 in the central stele establishes the strong basal auxin maximum required for root development. PIN1 apical polarity in the epidermis, as determined by the activity of the PINOID kinase and the colocalised NPH3-like protein ENHANCER OF PINOID (ENP), establishes the weaker auxin maxima required for the development of cotyledon primordia (Friml et al., 2003; Benková et al., 2003; Treml et al., 2005; Furutani et al., 2014).

Within 30 min after PBA treatment of ovules, confocal laser scanning microscopy (CLSM) showed that in 88% of *PIN1p:PIN1-GFP* embryos (n=33) there was a complete delocalisation of PIN1 in all cells including central stele cells (Fig. 5A-D; in 21/22 controls PIN1 linked to stele precursors was recognisable). After 48 h and 72 h, internal PIN1 was completely missing in the residual basal region of 90% of *mp* phenocopies (n=20; PIN1 present in all controls). Residual PIN1 remained in the upper cotyledon tissue, showing partial polarity in the central (vascular) tissue and full restoration in the epidermal tissue (Fig. 5E-H). PBA also caused irregularly developed cotyledon primordia (Fig. 5E-H, Fig. S7).

We then tested the dynamics of these proteins by time-limited immersion of ovules in PBA solutions. We focussed on epidermal and near-epidermal cells because these layers allow easy monitoring of protein-GFP localisation by CLSM. PBA treatment of *PIN1p: PIN1-GFP* or *35Sp:EGFP-ENP* embryos resulted in diffuse cytosolic internalisation of GFP signals (Fig. 5I,J). A similar effect was seen for ectopic EGFP-ENP in the root (Fig. 5K). In all cases internalisation could be significantly reversed after washing (Fig. 5I-L; for statistics see Table S6). Simultaneous staining with the PM marker FM4-64 showed only a few FM4-64 vesicles, excluding a general internalisation or perforation of the PM bi-layer under the conditions applied (Fig. 5M). Comparison with PIN2, a cortex- and epidermis-localised IAA efflux carrier that is not detectable in the embryo (Friml et al., 2003) but required in the post-embryonic root, did not show this marked internalisation (Fig. 5N; n=26). All applications were almost indistinguishable from each other in their effect, except a variable number of vesicles seen after 10 mM PBA (Fig. 5N,O), some of which merged with FM4-64 (Fig. 5O). Thus, PBA targets proteins involved in IAA transport differentially.

PBA suppresses the IAA-mediated degradation of DII-VENUS

IAA-triggered degradation of MP repressors, the Aux/IAA proteins, is known to release MP, which activates *PIN1*. We tested whether PBA could interfere with the degradation step in this regulatory
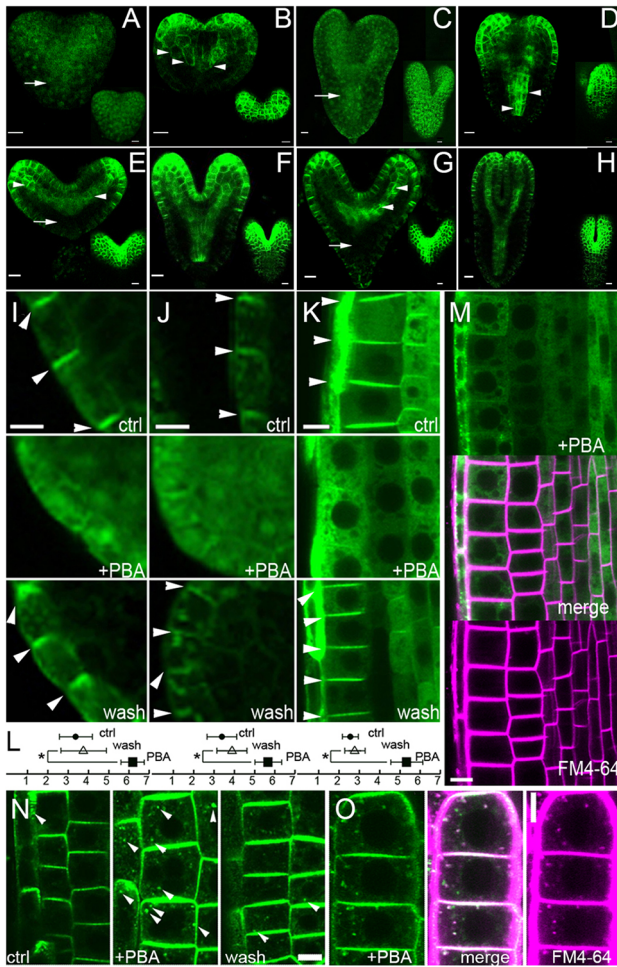

Fig. 5. Impact of PBA on membrane proteins. (A-D) *PIN1p:PIN1-GFP* embryos from isolated ovules treated with PBA (10 mM, 30 min; A,C) or water (30 min; B,D) and immediately analysed; (A,B) heart stage, (C,D) early torpedo stage. Note the diffuse GFP signals in A and C versus the membrane-localised signals in B and D. Internal views; arrows and arrowheads point to representative stele cells. Insets show surface views. (E-H) *PIN1p:PIN1-GFP* torpedo embryos from PBA (E,G) or water (F,H) treated siliques and analysed after 48 h (E,F) or 72 h (G,H). Note the absence of GFP signal in the residual basal tissue of *mp* phenocopies (arrows) versus its localisation in cotyledon tissue (arrowheads). Note the restoration of PIN1 polarity in epidermal cells of both treated and untreated embryos (insets). (I-K) Representative figures of embryo cotyledon and root tissue in control (ctrl), PBA treatment and wash experiments. Plants carry *35Sp:EGFP-ENP* (I,K) or *PIN1p:PIN1-GFP* (J). Arrowheads indicate polar protein localisation. (L) Semi-quantitative fluorescence analysis of PIN1-GFP and EGFP-ENP under PBA treatment, showing mean and s.d. for control (circle), PBA (square) and wash (triangle) treatments of the experiments in I-K (from left to right). *$P<0.001$, t-test (Table S6). The bottom bar with values 1-7 gives the categories of cellular signal distribution; about 2-4 for control, 2-5 for wash and 5-7 for PBA, indicating PM localisation in control and wash treatments and cytosolic distribution in PBA treatment. (M) *35Sp:EGFP-ENP* roots treated with PBA, counterstained with FM4-64, and merge. (N) *PIN2p:PIN2-GFP* roots in control, PBA treatment and wash. Arrowheads indicate small vesicles that are frequent in the PBA treatment. (O) *PIN2p:PIN2-GFP* roots treated with PBA, counterstained with FM4-64, and merge. Arrowheads indicate overlapping vesicles of GFP and FM4-64 fluorescence. Root tips are oriented to bottom. Scale bars: 10 μm in A-H; 5 μm in I-O.

circuit using the IAA signalling sensor DII-VENUS. This construct harbours a fluorescent protein fused to IAA-interaction domain II, which mediates Aux/IAA protein degradation (Brunoud et al., 2012). Application of PBA (10 mM) and IAA (10 μM) mixtures to roots of DII-VENUS plants (*n*=30) showed suppression of DII-VENUS degradation as compared with IAA treatment alone (Fig. 6; *n*=30). Water and PBA controls (*n*=30) showed signals comparable to those of the PBA/IAA co-treatment. Similar results were obtained with DII-VENUS using 1 μM IAA, whereas a resistant mutant mDII was not degraded by IAA (Fig. S8). Thus, PBA is able to directly or indirectly interfere with the step leading to BDL degradation.

PBA versus B competition causes PM accumulation of BOR1

In order to exclude or confirm a possible specificity of PBA for IAA-related embryo proteins we examined the root localisation of the B transporter BOR1, a PM protein unrelated to IAA transport. BOR1 function is directly linked to B homeostasis and shows a conspicuous response to cellular B concentration (Fig. 7, Figs S9 and S10). High concentrations of B, as given in MS media, lead to its endocytic degradation, whereas low concentrations lead to its accumulation (Takano et al., 2010). Seedlings carrying the *35Sp: BOR1-GFP* reporter were grown on 0.5MS for 10 days and then transferred for 2-3 days on H_2O-agar plates with low B concentration ('before', Fig. 7A). All showed high BOR1-GFP abundance in their root tips, as measured from the average fluorescence intensity. By contrast, subsequent incubation of the same seedlings in 0.5MS without sucrose (MS-S) and with 100 μM H_3BO_3 (MS-S+H_3BO_3) showed a reduced concentration of the fusion protein (Fig. 7B). Direct incubation in water or re-incubation of H_3BO_3-treated seedlings on water again displayed strong GFP signals ('+H_2O', Fig. 7C, Fig. S9). Surprisingly, incubation of roots in 0.5MS-S+H_3BO_3+PBA (100 μM, 10 mM) behaved like those in water (Fig. 7D). The difference to the MS-S+H_3BO_3 incubation was significant (*P*<0.001, *t*-test; Fig. 7E, Fig. S9, Table S7). Note that the cells of these roots encountered the same concentration of B as those without PBA. Essentially, the same picture emerged from experiments using B-depleted 0.5MS medium instead of a water incubation to challenge BOR1 expression (Fig. S10). These experiments also showed the effect of 0.5MS+H_3BO_3+PBA
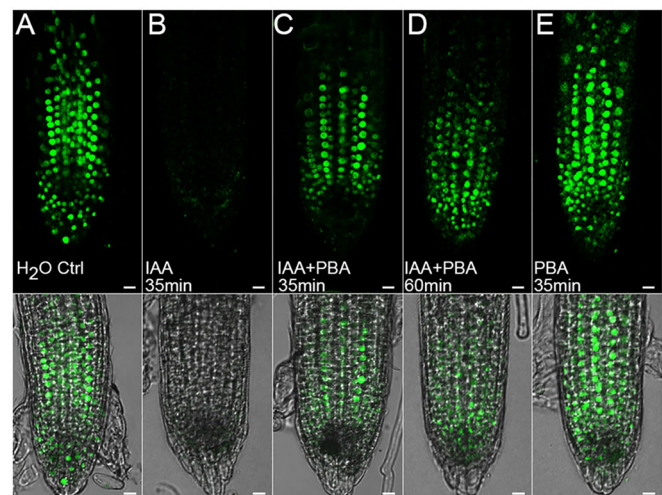

Fig. 6. The response of DII-VENUS to PBA and/or IAA. (A-E) Seedlings carrying the DII-VENUS construct were incubated in water (A), single (B,E) and combined (C,D) solutions of IAA (10 μM) and PBA (10 mM) for the indicated times. Top, VENUS fluorescence; bottom, merge of fluorescence signal and DIC. Scale bars: 10 μm.
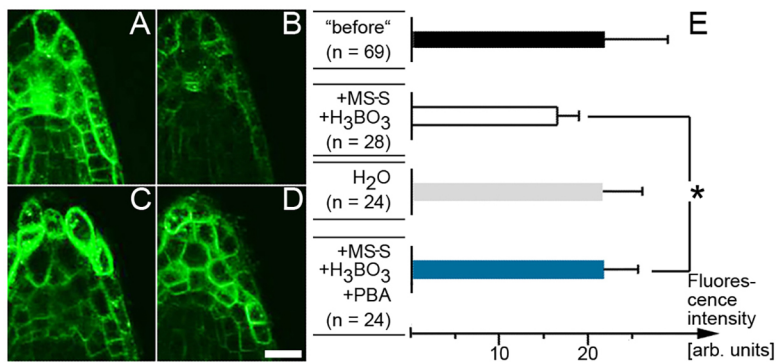
Fig. 7. B/PBA competition and BOR1 abundance. (A-D) Four representative root tips of *35Sp:BOR1-GFP* plants before treatment (A) and after incubation in 0.5MS-S+100 μM H_3BO_3 (B), in water (C) and in 0.5MS-S+100 μM H_3BO_3+10 mM PBA (D). (E) Estimated intensity values (mean and s.d.) for comparison of MS-S+H_3BO_3 versus MS-S+H_3BO_3+PBA treatments. *$P<0.001$, *t*-test (Table S7). Complete series is shown in Fig. S9. Scale bar: 10 μm.

versus 0.5MS($-H_3BO_3$)+PBA. In both cases BOR1 was expressed (Fig. S10, Table S8). Thus, PBA not only impacted on the localisation of particular IAA-related proteins but also on that of other PM proteins. The effect ranged from depletion (PIN1, ENP) to neutral impact (PIN2) to enhanced accumulation (BOR1).

DISCUSSION
Significance of the boronic acid moiety and molecular structure in the induction of *monopteros* phenocopies
Bassil et al. (2004) demonstrated that boronic acids and B compete for the same binding sites. However, competition experiments showed only a limited capability of increasing boric acid concentrations to restore PBA-inhibited pollen germination (Bassil et al., 2004). Using the 'silique system' presented in this study, the induction of PBA-induced *mp* phenocopies could not be convincingly suppressed with increasing amounts of boric acid (up to 150 mM). There are several likely reasons for this observation. Compared with boronic acids, boric acid has a higher pKa, indicating weaker dissociation and therefore affecting the strength to form ester bonds. Consequently, instead of flooding the cells with boric acid, washout of PBA is more suitable to revert its effects, such as the internalisation of ENP and PIN1. In this context, it is worth mentioning that PBA suppresses a known B effect by stabilising instead of internalising a membrane protein (BOR1). Also, a successful competition by boric acid has only a narrow time window during hypophysis division. Furthermore, the comparison of BBA with the other boronic acids suggests that molecular structure impacts the capability of a compound to penetrate tissues and to access its molecular targets, and thus to induce *mp* phenocopies. Apparently, boronic acids with a phenolic group outperform BBA with a carbon tail. In turn, boric acid might be even less able to penetrate through or access *cis*-diols at membranes. This problem cannot be circumvented using *A. thaliana* embryo culture because isolated embryos are not viable. However, these experiments helped to clarify another important question: the effect of BBA, when considered in terms of its structure, excluded the phenolic ring as causative for *mp* phenocopy induction. This was corroborated by the results obtained with all boronic acid 'analogues', which excluded the possibility that similar molecular structures were sufficient to induce phenocopies. Together, this showed that the ability to induce *mp* phenocopies is a property of the boronic acid moiety.

Boronic acid-induced PIN1 internalisation interrupts the IAA-driven MP/PIN1/TMO7 signal transduction loop causing *mp* phenocopy induction
Our data suggest a specific effect of PBA in the feedback signal transduction cascade leading to RAM development. All known

A. thaliana mutations causing *mp* or *mp*-like phenotypes map along this pathway (De Rybel et al., 2013; Schlereth et al., 2010; Hamann et al., 2002; Cheng et al., 2007; Friml et al., 2003).

In the early embryo, apical cells produce IAA (Wabnik et al., 2013), which triggers the degradation of Aux/IAA proteins, such as BDL, the repressors of MP (Fig. 8A). Released MP activates *TMO7*, *TMO5* and also *PIN1* in corresponding tissues (Schlereth et al., 2010; Hamann et al., 2002; De Rybel et al., 2013) and also impacts *ENP* expression (Furutani et al., 2014). Together, this establishes a feedback system because MP is itself dependent on IAA transported by PIN1. The steady-state flux of IAA from the source requires a continuous directional transport enabled by the polar localisation of PIN1 and regionally supported by proteins such as ENP (Friml et al., 2003; Benková et al., 2003; Treml et al., 2005; Furutani et al., 2014). This generates two weak auxin maxima for the cotyledon primordia and a strong auxin maximum in the hypophysis cell. The strong auxin maximum and TMO7 (coming from the central cells) signal to induce the formative horizontal division of the hypophysis (Fig. 8A).

In this scenario, internalisation of PIN1 by PBA blocks IAA transport to and from central cells and causes the loss of the root auxin maximum and MP activity due to failure of IAA-mediated degradation of BDL (Fig. 8B). Consequently, the expression of *TMO7* and *PIN1* is also abolished, as in *mp* mutants (Fig. 8B). Regionally, this also impacts the presence of TMO5. In the apex, internalised PIN1 and ENP cause a disturbance of IAA transport, as manifested in abnormalities in cotyledon maxima and cotyledon growth. Note that endogenously synthesized IAA enables MP release and activity, which explains, at least partially, *TMO5* expression in PBA-induced *mp* phenocopies, which have an intact *MP* gene, in contrast to *mp* mutants (Fig. 8B).

However, the response of the DII-VENUS construct to PBA/IAA is also compatible with an alternative model whereby PBA has a direct inhibitory role, suppressing IAA-mediated BDL degradation and ultimately inducing *mp* phenocopies (Fig. 8B). It remains to be determined whether this DII-VENUS response could also result from a rapid PBA-induced rearrangement of membrane transport systems, precluding effective penetration by IAA. The effect of PBA on another transport system (BOR1) rather supports a more general effect of PBA on PM proteins.

The restoration of (epidermal) PIN1 polarity after 48 h demonstrates the transient impact of the early PBA pulse, validating PBA as a tool to analyse the significance of timing in development. It shows that a transient interruption of RAM formative divisions is sufficient to prevent embryonic root development completely. It is not possible to draw such a conclusion from the study of mutants, which constantly lack MP function.
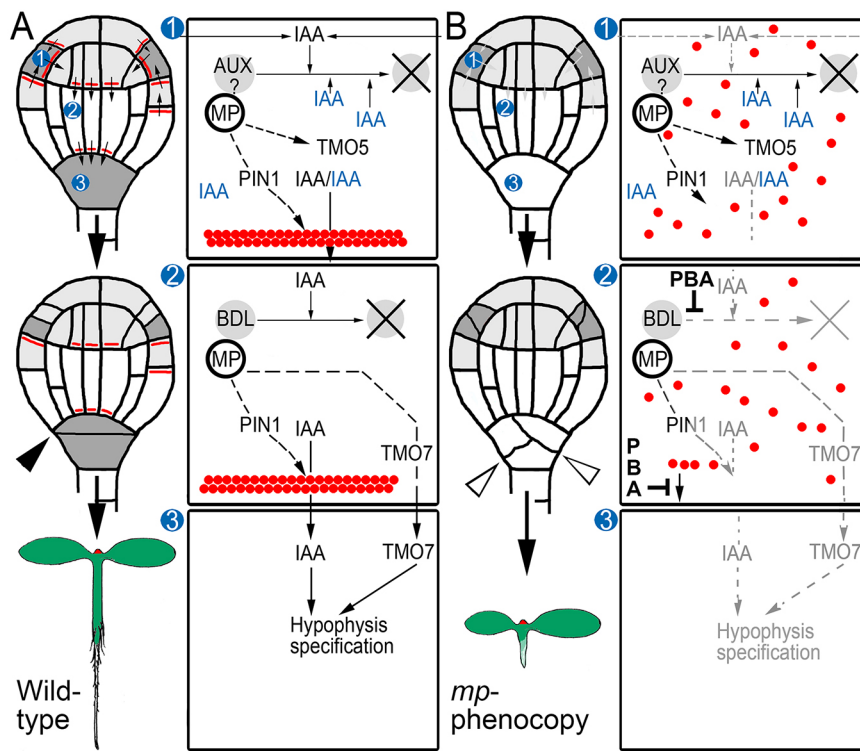
Fig. 8. Model of induction of the *mp* phenocopy by PBA in the embryo. (A) Shown are the molecular processes of IAA-driven signal transduction in apical cells (1), central vascular precursor cells (2) and the hypophysis (3) in the development of a globular embryo into a seedling (top to bottom; see Schlereth et al., 2010). (B) PBA-induced effects in cells 1, 2 and 3 as in A. Apical cells (grey) are sources of IAA. IAA transport (small arrows) by PIN1 (red circles) establishes apical and basal IAA maxima (dark grey). Endogenous IAA, blue; transported IAA, black; AUX, local Aux/IAA repressor; BDL, central vascular cell Aux/IAA repressor; black arrowhead, normal asymmetric division of the hypophysis; small black versus small grey arrows, normal versus disturbed IAA transport; open arrowheads, irregular cell divisions of the hypophysis. Possible interferences by PBA are indicated. For details see main text.

There are interesting parallels between the induced loss of an embryonic root and the halted post-embryonic root development in other plants, although both root forms also have significant differences (e.g. weak embryonic BOR1 expression in the former; GENEVESTIGATOR database and our unpublished data). Sunflower, field bean and *A. thaliana* respond with partial or complete reduction of RAM activity when grown on B-deficient soil or media (Parr and Loughman, 1983; Dell and Huang, 1997; Martin-Rejano et al., 2011; Abreu et al., 2014; Li et al., 2015). *A. thaliana* also shows a reduction of localised PIN1 in the stele (Li et al., 2015). However, these effects result from long-term growth, in contrast to the rapid responses to transient PBA application.

The specific effects of PBA suggest a role for B in membrane generation and/or maintenance

Excess or reduction of B, as well as the presence of boronic acids (which mimic B depletion), can cause various physiological effects *in vitro* and *in vivo* ranging from abnormal gene splicing and expression to variable plant growth and lethality (e.g. Sommer and Sorokin, 1928; Kliegel, 1980; Parr and Loughman, 1983; Shorrocks, 1997; Dell and Huang, 1997; Goldbach et al., 2001; Shomron and Ast, 2003; Reid et al., 2004; Bassil et al., 2004; Martin-Rejano et al., 2011; Abreu et al., 2014; Durbak et al., 2014). However, under the conditions applied, PBA demonstrated an intriguing specificity on a morphological, cellular and also molecular level as evidenced by its variable but specific effects on four different PM proteins (PIN1, ENP, PIN2 and BOR1). This might indicate that disturbance of the B/*cis*-diol cross-links themselves could be part of a cellular B sensing mechanism, explaining why, in the presence of PBA, the cells do not respond to high cellular B levels.

PIN1-driven IAA transport might also be affected in *Eranthis hyemalis*, where PBA-induced monocotyly (Haccius, 1960) is likely to be a reflection of its unusual mode of development. At present, the PBA targets in these processes are not known,

although plants possess numerous potential glycosylated targets, some with known morphogenetic impact (Motose et al., 2004; Geshi et al., 2013; Voxeur and Fry, 2014). Plants might also have N- and O-linked glycosylated protein sorting codes, as known from animals (Mellman and Nelson, 2008). In either case, the observations presented in the current study are of prime importance in our understanding of membrane structure. The combination of all PBA-specific effects supports the long-standing hypothesis that B has a functional role in membrane architecture. This finding in plant embryos might point to a comparable role in animals, which display B-related embryo defects but lack a cell wall (Lanoue et al., 1998; Rowe and Eckert, 1999; Fort et al., 2002).

MATERIALS AND METHODS

Plant material, growth and treatment of siliques with boronic acids, acetic acids and benzoic acids

As wild types, Columbia (Col-0) and Landsberg *erecta* (L*er*-0) were used. Mutants were *mp*-B4149 (Schlereth et al., 2010) and *bdl* (without designation, courtesy of G. Jürgens, University of Tübingen, Germany). Routinely, all siliques of a stem/branch and (often) the first three flowers were thoroughly coated (~10-15 times) with the corresponding solution using a brush. Treated flowers eventually produced seeds or became necrotic. Plants were treated only once, except in one series with a single treatment per day on five consecutive days. The seeds of untreated terminal flower buds of the same stem and/or a different stem, and seeds from siliques of separated plants treated with water were harvested as controls. For additional BBA treatments, siliques were opened laterally with microsurgical forceps (Fine Science Tools). Plants were grown under conditions as previously described (Treml et al., 2005) and siliques were separately harvested. For ovule culture, siliques were opened and fixed on surface-sterilised slides with double adhesive tape. Ovules were covered for 5 or 10 min with PBA (5 mM), BBA (50 mM in 0.1% DMSO) and water as control and then transferred to medium and cultured as previously described (Sauer and Friml, 2004). For short-term analysis (shown Fig. 5A-D), ovules were covered in 10 mM PBA for 30 min and then immediately analysed by CLSM.

Chemicals

Except for PBA (Merck), all compounds were obtained from Sigma-Aldrich. Unless stated otherwise, solutions were prepared in water. A series of experiments revealed satisfactory induction frequencies of *mp* phenocopies with 50 mM PBA (for instance, 10 mM produces fewer than 5% phenocopies). Where possible, 50 mM concentrations were adjusted for the correspondingly tested compounds. In the case of 3-nitrophenylboronic acid, 4-methoxyphenylacetic acid, 3-nitrophenylacetic acid, 3-methoxybenzoic acid, 4-methoxybenzoic acid and 3-nitrobenzoic acid, saturated solutions were used because 50 mM surpassed the corresponding solubilisation capacity.

RT-PCR analyses

Total RNA isolation, reverse transcription, PCR and purification of amplification products of material of wild types, induced *mp* phenocopies, boronic acid-treated seedlings of wild-type appearance, and *mp* or *bdl* mutants were performed according to conventional methods (Treml et al., 2005). Amplification products were sequenced through Eurofins/MWG services. Primers (5′-3′, forward and reverse) were: *ACT2*, TTGTTCCAGCCCTCG-TTTGT and CCTGGACCTGCCTCATCATACT; *TMO5*, ATGTACGC-AATGAAAGAAGA and ATTATAACATCGATTCACCA; *TMO7*, ATGTCGGGAAGAAGATCACG and TTGGGTAAGTAAGCTTCTGA.

Microscopy

Whole-mounts and semi-thin sections were prepared as previously described (Haberer et al., 2002; Treml et al., 2005). High-magnification images of seedlings were taken with a Hitachi TM3000 table-top microscope.

Epifluorescence of embryos carrying *GFP* constructs was analysed 24-72 h after treatment of siliques with 50 mM PBA using a Zeiss Axiophot 1 or an Olympus BX61 microscope.

The dynamics of reversible PM protein localisation was analysed by CLSM of embryos carrying PIN1-GFP or EGFP-ENP reporter. Initial experiments revealed that higher (mM) PBA concentrations led to necrosis and death of isolated embryos, whereas lower (μM) concentrations had no effect even after hours. Empirically, the best results were obtained when ovules of 10-15 siliques were collected in water purified through Millipore columns (mQ water) and then incubated for 15 min in 25 mM PBA (ENP) or for 10 min in 30 mM PBA (PIN1); PBA was dissolved in mQ water. A small fraction of the initial collection of ovules was kept in mQ water for the duration of the whole experiment as an experimental control. After incubation, an aliquot of embryos, released from the ovules by pressing the coverslip, was checked by CLSM. The remaining ovules were washed three times with mQ water and then left for washout in mQ water for 2 h. Then, this washout fraction and the experimental control embryos were analysed by CLSM. The quality of the embryos in the experimental control was decisive for evaluating the experiment. If the quality was not sufficient (e.g. as shown by poor retention of proteins at the PM, visible necrosis), the complete experiment was repeated. For embryo and root analyses, epidermal cells were best suited.

For the analysis of roots (ENP, PIN2), initially 24 seedlings were collected in 0.5MS without sucrose (MS-S); then, 16 seedlings were incubated in 10 mM PBA for 30 min in two independent experimental series and for 60 min in another experiment. The remaining 8 seedlings remained for the duration of the whole experiment in 0.5MS-S (experimental control). After incubation, 8 seedlings were counterstained with FM4-64 and analysed by CLSM. The remaining 8 seedlings were washed three times with 0.5MS-S and then left for washout in 0.5MS-S for 2 h. The washout fraction and the experimental control were counterstained with FM4-64 and analysed by CLSM.

For CLSM analysis, we used an Olympus LSM FV100 and associated FluoView software. Images were taken of epidermal cells (embryos) and of transverse optical sections (roots) of epidermal cells in the area where the lateral root cap ends. Excitation of GFP and VENUS probes at 488 nm and 515 nm, respectively, was with a multiline argon laser (500-550 nm and 500-600 nm slit width, respectively). For embryo analyses the laser intensity was kept at 10-15%, for root images at 1% (PIN2: HV, 550; gain, 1; offset, −3) or 0.5% (ENP: HV, 500; gain, 1; offset, −3) and the images were

acquired with a high-sensitivity GaAsp detector unit (Olympus). One-way scan images (Kahlman frame) were obtained using an Olympus Plan APO 60× water objective. Excitation of FM4-64 was at 561 nm and the laser intensity was kept at 0.9% (HV, 538; gain, 1; offset, 5).

PBA versus boric acid competition experiments using *BOR1-GFP* plants

We considered that accumulation of the B transporter BOR1 is controlled by the B conditions (Takano et al., 2010, 2005; Kasai et al., 2011; Yoshinari et al., 2012).

Seedlings carrying *35Sp:BOR1-GFP* were surface sterilised and grown for 10 days on sterile 0.5MS plates. The subsequent transfer onto H_2O-agar plates for 2-3 days led to significant enhancement of BOR1-GFP fluorescence (Fig. 7, Figs S9 and S10). For each experiment between 8 and 24 seedlings were prechecked by CLSM. Then 8 seedlings each (only 4 seedlings in the case of experiment no.2) were transferred for 2 h into different solutions. The basic 0.5MS used for these incubations was without sucrose and without H_3BO_3. If present in the medium, B was always adjusted with H_3BO_3 to 100 μM final and PBA was adjusted to 10 mM. Collectively, four different conditions were analysed: directly after growth on H_2O-agar plates ('before') and after incubation in 0.5MS-S/+H_3BO_3, water (mQ) or 0.5MS-S/+H_3BO_3/+PBA medium. Four independent experiments were performed (Fig. S9). After incubation, the GFP fluorescence of the seedlings was documented by CLSM (laser 488 nm; intensity, 1%; HV, 530; gain, 1; offset, −3). In three experiments we also tested the response of roots incubated in 0.5MS-S/+H_3BO_3 by recultivating them on H_2O-agar plates overnight. Most of these root tips displayed stronger fluorescence than with 0.5MS-S/+H_3BO_3 incubation alone (Fig. S9).

In an additional experimental series the water (mQ) treatment was replaced by incubation in 0.5MS without sucrose and H_3BO_3 (0.5MS-S/-H_3BO_3) and further incubations were in 0.5MS-S/+H_3BO_3, 0.5MS-S/+H_3BO_3/+PBA or 0.5MS-S/+PBA (Fig. S10). Seedlings with obvious root defects were discarded from further analysis. For fluorescence intensity quantification the images were cropped using GIMP software (www.gimp.org) and intensities were measured using Fiji software (Schindelin et al., 2012). The significance of intensity differences was assessed by *t*-test (see below; Tables S7 and S8). For better display, brightness was increased for all cropped images to the same extent (Figs S9 and S10).

Semi-quantitative analysis of fluorescence signals in PBA-treated embryos and root

The depletion of the PM from proteins (EGFP-ENP, PIN1-GFP) is not always complete, for instance because some cells of embryos and roots are injured during the isolation and transfer procedures; also, it is unlikely that all tissue parts contact the compound to the same extent, and the same holds true for the washing steps. Therefore, we assessed the distribution of GFP signals in a semi-quantitative way by estimating the extent of cytosolic versus PM fluorescence signal for epidermal cells by eye. For each reporter gene (*EGFP-ENP*, *PIN1-GFP*) and tissue (embryo, root) at least three independent experiments were performed. Four persons (the authors, two technicians) independently rated CLSM images of embryo and root epidermal cells (see Table S6). Depending on the quality of the image, 3-12 cells per image (equals one data point) were evaluated (Table S6). Therefore, single data points in Table S6 take fractions and not positive integers. We established four intensity classes or categories for cytosol (C0-C3) and the PM (P0-P3). Instead of separating 16 different classes, we established seven different groups: P3C0 (no.1; indicates complete localisation at the PM); the combined groups P3C1/P2C0 (no.2), P3C2/P2C1/P1C0 (no.3), P3C3/P2C2/P1C1/P0C0 (no.4), P2C3/P1C2/P0C1 (no.5), P1C3/P0C2 (no.6); and P0C3 (no.7; indicates exclusive localisation in the cytosol).

Statistics

For statistical analyses we used Excel (Microsoft) or Prism (GraphPad) software. The data groups of the 0.5MS-S/+H_3BO_3 versus 0.5MS-S/+H_3BO_3/PBA experiments of *35S:BOR1::GFP* plants could be directly analysed (Tables S7 and S8). The data of the cytosolic versus PM

comparison of EGFP-ENP and PIN1-GFP in PBA-treated versus washed material required an additional step: here, prior to further processing, the mean of three independent assessments (see above, semi-quantitative analysis of fluorescence signals) was determined (Table S6).

The data groups to be subjected to (two-tailed) *t*-tests were first analysed for Gaussian distribution with a Kolmogorov–Smirnov (KS) test. All data groups passed a first KS test except that of the EGFP-ENP wash experiment. For this group, a KS test with Bonferroni correction for multiple tests showed that the assumption of a normal distribution was not rejected at a significance level of 5%. Thus, all experimental comparisons could be analysed with (two-tailed) *t*-tests to assess whether the differences in root and embryo experiments were significant (see Figs 5, 7, Figs S9, S10, Tables S6-S8).

Author contributions
M.M. performed, assessed and validated applications with boronic, benzoic and acetic acid, molecular work, electron microscopy and CLSM work, figures showing fluorescent images and statistics. R.A.T.-R. designed the project, performed the other applications, histological sections, embryo analyses (Nomarski, epifluorescence microscopy), participated in CLSM work (Fig. 5A-H, Fig. 6) and statistics, and wrote the paper.

Supplementary information
Supplementary information available online at
http://dev.biologists.org/lookup/doi/10.1242/dev.131375.supplemental

References
Abreu, I., Poza, L., Bonilla, I. and Bolaños, L. (2014). Boron deficiency results in early repression of a cytokinin receptor gene and abnormal cell differentiation in the apical root meristem of *Arabidopsis thaliana*. *Plant Physiol. Biochem.* **77**, 117-121.

Bassil, E., Hu, H. and Brown, P. H. (2004). Use of phenylboronic acids to investigate boron function in plants. Possible role of boron in transvacuolar cytoplasmic strands and cell-to-wall adhesion. *Plant Physiol.* **136**, 3383-3395.

Benková, E., Michniewicz, M., Sauer, M., Teichmann, T., Seifertová, D., Jürgens, G. and Friml, J. (2003). Local, efflux-dependent auxin gradients as a common module for plant organ formation. *Cell* **115**, 591-602.

Bolaños, L., Lukaszewski, K., Bonilla, I. and Blevins, D. (2004). Why boron? *Plant Physiol. Biochem.* **42**, 907-912.

Brown, P. H., Bellaloui, N., Wimmer, M. A., Bassil, E. S., Ruiz, J., Hu, H., Pfeffer, H., Dannel, F. and Römheld, V. (2002). Boron in plant biology. *Plant Biol.* **4**, 205-223.

Brunoud, G., Wells, D. M., Oliva, M., Larrieu, A., Mirabet, V., Burrow, A. H., Beeckman, T., Kepinski, S., Traas, J., Bennett, M. J. et al. (2012). A novel sensor to map auxin response and distribution at high spatio-temporal resolution. *Nature* **482**, 103-106.

Chen, X., Schauder, S., Potier, N., Van Dorsselaer, A., Pelczer, I., Bassler, B. L. and Hughson, F. M. (2002). Structural identification of a bacterial quorum-sensing signal containing boron. *Nature* **415**, 545-549.

Cheng, Y., Dai, X. and Zhao, Y. (2007). Auxin synthesized by the YUCCA flavin monooxygenases is essential for embryogenesis and leaf formation in *Arabidopsis*. *Plant Cell* **19**, 2430-2439.

De Rybel, B., Möller, B., Yoshida, S., Grabowicz, I., de Reuille, P. B., Boeren, S., Smith, R. S., Borst, J. W. and Weijers, D. (2013). A bHLH complex controls embryonic vascular tissue establishment and indeterminate growth in *Arabidopsis*. *Dev. Cell* **24**, 426-437.

Dell, B. and Huang, L. (1997). Physiological response of plants to low boron. *Plant Soil* **193**, 103-120.

Durbak, A. R., Phillips, K. A., Pike, S., O'Neill, M. A., Mares, J., Gallavotti, A., Malcomber, S. T., Gassmann, W. and McSteen, P. (2014). Transport of boron by the tassel-less1 aquaporin is critical for vegetative and reproductive development in maize. *Plant Cell* **26**, 2978-2995.

Fort, D. J., Rogers, R. L., McLaughlin, D. W., Sellers, C. M. and Schlekat, C. L. (2002). Impact of boron deficiency on *Xenopus laevis. Biol. Trace Element Res.* **90**, 117-142.

Friml, J., Vieten, A., Sauer, M., Weijers, D., Schwarz, H., Hamann, T., Offringa, R. and Jürgens, G. (2003). Efflux-dependent auxin gradients establish the apical-basal axis of *Arabidopsis*. *Nature* **426**, 147-153.

Furutani, M., Nakano, Y. and Tasaka, M. (2014). MAB4-induced auxin sink generates local auxin gradients in *Arabidopsis* organ formation. *Proc. Natl. Acad. Sci. USA* **111**, 1198-1203.

Geshi, N., Johansen, J. N., Dilokpimol, A., Rolland, A., Belcram, K., Verger, S., Kotake, T., Tsumuraya, Y., Kaneko, S., Tryfona, T. et al. (2013). A galactosyltransferase acting on arabinogalactan protein glycans is essential for embryo development in *Arabidopsis*. *Plant J.* **76**, 128-137.

Goldbach, H. E. and Wimmer, M. A. (2007). Boron in plants and animals: is there a role beyond cell-wall structure? *J. Plant Nutr. Soil Sci.* **170**, 39-48.

Goldbach, H. E., Yu, Q., Wingender, R., Schulz, M., Wimmer, M., Findeklee, P. and Baluška, F. (2001). Rapid response reactions of roots to boron deprivation. *J. Plant Nutr. Soil Sci.* **164**, 173-181.

Haberer, G., Erschadi, S. and Torres-Ruiz, R. A. (2002). The Arabidopsis gene PEPINO/PASTICINO2 is required for proliferation control of meristematic and non-meristematic cells and encodes a putative anti-phosphatase. *Dev. Genes Evol.* **212**, 542-550.

Haccius, B. (1960). Experimentell induzierte Einkeimblättrigkeit bei *Eranthis hiemalis. Planta* **54**, 482-497.

Hamann, T., Benkova, E., Bäurle, I., Kientz, M. and Jürgens, G. (2002). The *Arabidopsis* BODENLOS gene encodes an auxin response protein inhibiting MONOPTEROS-mediated embryo patterning. *Genes Dev.* **16**, 1610-1615.

Ishii, T. and Matsunaga, T. (1996). Isolation and characterization of a boron-rhamnogalacturonan-II complex from cell walls of sugar beet pulp. *Carbohydr. Res.* **284**, 1-9.

Jürgens, G. and Mayer, U. (1994). *Arabidopsis*. In *Embryos. Colour Atlas of Development* (ed. J. B. L. Bard), pp. 7-21. London: Wolfe Publishing.

Kasai, K., Takano, J., Miwa, K., Toyoda, A. and Fujiwara, T. (2011). High boron-induced ubiquitination regulates vacuolar sorting of the BOR1 borate transporter in *Arabidopsis thaliana*. *J. Biol. Chem.* **286**, 6175-6183.

Kliegel, W. (1980). *Bor in Biologie, Medizin und Pharmazie*. Berlin: Springer.

Kobayashi, M., Matoh, T. and Azuma, J. (1996). Two chains of rhamnogalacturonan II are cross-linked by borate-diol ester bonds in higher plant cell walls. *Plant Physiol.* **110**, 1017-1020.

Lanoue, L., Taubeneck, M. W., Muniz, J., Hanna, L. A., Strong, P. L., Murray, F. J., Nielsen, F. H., Hunt, C. D. and Keen, C. L. (1998). Assessing the effects of low boron diets on embryonic and fetal development in rodents using in vitro and in vivo model systems. *Biol. Trace Elem. Res.* **66**, 271-298.

Li, K., Kamiya, T. and Fujiwara, T. (2015). Differential roles of PIN1 and PIN2 in root meristem maintenance under low-B conditions in *Arabidopsis thaliana*. *Plant Cell Physiol.* **56**, 1205-1214.

Martin-Rejano, E. M., Camacho-Cristobál, J. J., Herrera-Rodriguez, M. B., Rexach, J., Navarro-Gochicoa, M. T. and Gonzalez-Fontes, A. (2011). Auxin and ethylene are involved in the responses of root system architecture to low boron supply in *Arabidopsis* seedlings. *Physiol. Plantarum* **142**, 170-178.

Mellman, I. and Nelson, W. J. (2008). Coordinated protein sorting, targeting and distribution in polarized cells. *Nat. Rev. Mol. Cell Biol.* **9**, 833-845.

Motose, H., Sugiyama, M. and Fukuda, H. (2004). A proteoglycan mediates inductive interaction during plant vascular development. *Nature* **429**, 873-878.

Nielsen, F. H. (2008). Is boron nutritionally relevant? *Nutr. Rev.* **66**, 183-191.

O'Neill, M. A., Warrenfeltz, D., Kates, K., Pellerin, P., Doco, T., Darvill, A. G. and Albersheim, P. (1996). Rhamnogalacturonan-II, a pectic polysaccharide in the walls of growing plant cell, forms a dimer that is covalently cross-linked by a borate ester. In vitro conditions for the formation and hydrolysis of the dimer. *J. Biol. Chem.* **271**, 22923-22930.

Park, M., Li, Q., Shcheynikov, N., Zeng, W. and Muallem, S. (2004). NaBC1 is a ubiquitous electrogenic Na+-coupled borate transporter essential for cellular boron homeostasis and cell growth and proliferation. *Mol. Cell* **16**, 331-341.

Parr, A. J. and Loughman, B. C. (1983). Boron and membrane function in plants. In *Metals and Micronutrients* (ed. D. A. Robb and W. S. Pierpoint), pp. 87-107. London: Academic Press.

Reid, R. J., Hayes, J. E., Post, A., Stangoulis, J. C. R. and Graham, R. D. (2004). A critical analysis of the causes of boron toxicity in plants. *Plant Cell Environ.* **27**, 1405-1414.

Rowe, R. I. and Eckhert, C. D. (1999). Boron is required for zebrafish embryogenesis. *J. Exp. Biol.* **202**, 1649-1654.

Sauer, M. and Friml, J. (2004). *In vitro* culture of *Arabidopsis* embryos within their ovules. *Plant J.* **40**, 835-843.

DEVELOPMENT

Schindelin, J., Arganda-Carreras, I., Frise, E., Kaying, V., Longair, M., Pietzsch, T., Preibisch, S., Rueden, C., Saalfeld, S., Schmid, B. et al. (2012). Fiji: an open-source platform for biological-image analysis. *Nat. Methods* **9**, 676-682.

Schlereth, A., Möller, B., Liu, W., Kientz, M., Flipse, J., Rademacher, E. H., Schmid, M., Jürgens, G. and Weijers, D. (2010). MONOPTEROS controls embryonic root initiation by regulating a mobile transcription factor. *Nature* **464**, 913-916.

Shomron, N. and Ast, G. (2003). Boric acid reversibly inhibits the second step of pre-mRNA splicing. *FEBS Lett.* **552**, 219-224.

Shorrocks, V. M. (1997). The occurrence and correction of boron deficiency. *Plant Soil* **193**, 121-148.

Simon, S. and Petrásek, J. (2011). Why plants need more than one type of auxin. *Plant Sci.* **180**, 454-460.

Sommer, A. L. and Sorokin, H. (1928). Effects of the absence of boron and of some other essential elements on the cell and tissue structure of the root tips of *Pisum sativum. Plant Physiol.* **3**, 237-260.

Takano, J., Noguchi, K., Yasumori, M., Kobayashi, M., Gajdos, Z., Miwa, K., Hayashi, H., Yoneyama, T. and Fujiwara, T. (2002). *Arabidopsis* boron transporter for xylem loading. *Nature* **420**, 337-340.

Takano, J., Miwa, K., Yuan, L., von Wirén, N. and Fujiwara, T. (2005). Endocytosis and degradation of BOR1, a boron transporter of Arabidopsis thaliana, regulated by boron availability. *Proc. Natl. Acad. Sci. USA* **102**, 12276-12281.

Takano, J., Tanaka, M., Toyoda, A., Miwa, K., Kasai, K., Fuji, K., Onouchi, H., Naito, S. and Fujiwara, T. (2010). Polar localization and degradation of *Arabidopsis* boron transporters through distinct trafficking pathways. *Proc. Natl. Acad. Sci. USA* **107**, 5220-5225.

Tanaka, M., Wallace, I. S., Takano, J., Roberts, D. M. and Fujiwara, T. (2008). NIP6;1 is a boric acid channel for preferential transport of boron to growing shoot tissues in *Arabidopsis. Plant Cell* **20**, 2860-2875.

Torssell, K. (1963). Action of some organoboron compounds on wheat roots and on pollen and distribution of C^{14} labelled benzeneboronic acid in plants. *Phys. Plantarum* **16**, 92-103.

Treml, B. S., Winderl, S., Radykewicz, R., Herz, M., Schweizer, G., Hutzler, P., Glawischnig, E. and Torres-Ruiz, R. A. (2005). The gene *ENHANCER OF PINOID* controls cotyledon development in the *Arabidopsis* embryo. *Development* **132**, 4063-4074.

Voxeur, A. and Fry, S. C. (2014). Glycosylinositol phosphorylceramides from *Rosa* cell cultures are boron-bridged in the plasma membrane and form complexes with rhamnogalacturonan II. *Plant J.* **79**, 139-149.

Wabnik, K., Robert, H. S., Smith, R. S. and Friml, J. (2013). Modeling framework for the establishment of the apical-basal embryonic axis in plants. *Curr. Biol.* **23**, 2513-2518.

Warington, K. (1923). The effect of boric acid and borax on the broad bean and certain other plants. *Ann. Bot.* **27**, 630-672.

Wimmer, M. A., Lochnit, G., Bassil, E., Mühling, K. H. and Goldbach, H. E. (2009). Membrane-associated, boron-interacting proteins isolated by boronate affinity chromatography. *Plant Cell Physiol.* **50**, 1292-1304.

Yan, J., Springsteen, G., Deeter, S. and Wang, B. (2004). The relationship among pKa, pH, and binding constants in the interactions between boronic acids and diols – it is not as simple as it appears. *Tetrahedron* **60**, 11205-11209.

Yoshinari, A., Kasai, K., Fujiwara, T., Naito, S. and Takano, J. (2012). Polar localization and endocytic degradation of a boron transporter, BOR1, is dependent on specific tyrosine residues. *Plant Signal. Behav.* **7**, 46-49.

DEVELOPMENT